Algorithms and ideas on measuring 3D particles with cost efficient hardware

Peter Frühberger

Vision and Fusion Laboratory
Institute for Anthropomatics
Karlsruhe Institute of Technology (KIT), Germany
peter.fruehberger@kit.de

Technical Report IES-2015-11

Abstract: Measuring the volume of dirt particles within the context of technical cleanliness is an important task. The estimated 3D shape yields significant information about material properties and can highlight potential risks while using the produced goods within the final product. The results of this analysis are used to optimize the production steps to eliminate such harmfully shaped particles already in the early stages. Estimating 3D volume of particles with just a few microns of surface area normally implies an expensive microscope measuring device. This report investigates on hardware and software approaches to implement a cost efficient sensor consisting of standard components. A hardware setup using eight LED lights for illuminating the specimen from various known directions while using the shadow casts to reconstruct the object surface are proposed and evaluated. By manipulating the intensity of these LEDs the setup can be adjusted to be useful for various specimen with different reflection properties. The height of a particle is estimated at discrete positions based on a global model. Measurement results acquired by established state-of-the-art microscopes are analyzed for incorporation into the donated model for initial ground-truth. During the calibration process those results are used to map measured height values to the scalar z-values used for height estimation of the given specimen.

1 Introduction

Technical cleanliness is used to document and identify contamination on produced parts and surfaces. Quality assurance in other applications is directly applied on the examined object with optical or tactile measurement devices like camera systems, light-microscopy and interferometry. In technical cleanliness this approach is not feasible, because the particles of interest are not visible from the outside. Engine blocks, tubes and closed housings need special constructions and automation solutions in order to examine these goods with given measurement sensors directly. Therefore an intermediate step for extracting the particles out of the specimen (extraction) is introduced [dA14]. The part is washed with e.g. demineralized or alcohol assorted water and the outflow is filtered. The contamination in form of dirt particles is examined with given inspection devices after this extraction. Depending on the optical contrast conditions, filter material and dirt particle properties, the filter needs to be dried in a further post-processing step. Figure 1.1 is illustrating where the initial extraction process takes place.

There are different particles to be measured as shown in Figure 1.1. This non complete selection of different particle-types outlines several problems. Threads as seen in Figure 1.2(c) need to be unwrapped and their length needs to be estimated. Because of the extraction process, particles might conglomerate. This puts high demands on the software algorithms to segment the particle from the background and to segment the particles from each other 1.2(b). In this report we concentrate on single particles, well separated from the background by using established segmentation methods, as we are interested in finding an estimation of particle's height. Though the lateral dimensions are also relevant as the shape of the particle is needed to segment it from the background.

(a)

(b)

Figure 1.1: In the extraction step dirt particles are washed out of the examined technical good (a). A complete cleaning setup can be seen in (b). Images source: Gläser Company (Horb).

(a) (b) (c)

Figure 1.2: An overview acquired with a Leica Z-16 microscope is shown on (a). A detailed view of a conglomerate of particles in (b). It is further mandatory to unwrap eventual threads as seen in (c).

Estimating volume and 3D shape of dirt particles in the context of technical cleanliness is a crucial task as it yields important information concerning the risks such particles might cause inside technical components. [dA14] defines particles within a range of 50 to 1000 μm diameter as mandatory to be detectable. The inspection system therefore needs to provide a sufficient acquisition resolution and suitable optical properties like depth of focus in combination with a movable z-axis to reconstruct height information as shown in [FKB14]. A typical particle filter has a diameter of around 7 cm, which makes a moving table mandatory when examining the complete filter. Though estimation of 3D shape and volume is not yet a mandatory specification demanded by the standards [dA14], it is quite clear that the impact of harmful shaped particles occurring as conglomerations emerged by accumulations in the use-case scenario is quite considerable. Because of this reason 3D shape measurement and volume estimation was added into the appendix of the above specification and is likely to be mandatory in upcoming revisions.

This technical report describes an image processing approach in combination with a developed hardware illumination for detecting and analyzing clotted residuals on particle filters after the initial extraction and drying process as seen in figure 1.2. Those ideas were summarized and presented at the 3rd International Multidisciplinary Microscopy and Microanalysis Conference in October 2015 [FSB16]. This report at hand extends these results and examines the robustness of the described approach. It also presents errors in the volume estimation when shadow detection fails through misinterpretation of contours or noise in the acquired image. It formulates ideas to limit regions with suitable shadow per particle out of given geometry.

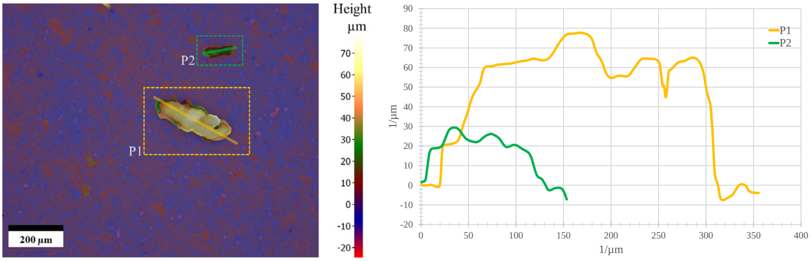

(a) (b)

Figure 1.3: Alicona InfinitFocus reconstruction of the lateral area shown as 2.5D (a) and the corresponding profile of the selected particles (b).

Figure 1.3 is showing a randomly selected particle filter analyzed with an Alicona InfinitFocus microscope. It can be seen, that estimating height information is a demanding task even for specialized measurement devices. The height of one of the particles seen in 1.3(a) is around 20 μm. Imitating professional measurement devices by replicating such a depth from focus setup is not feasible from a cost-efficient point of view, as accurate, e.g. a few microns moving z-axis within a low uncertainty level are expensive. Furthermore the optical lenses needed would be counterproductive against the need to examine a rather large lateral area.

1.1 Experimental setup and software implementation

The experimental setup consists of three components, a custom-built double LED ring light in combination with an industrial camera equipped with a bi-telecentric objective lens. The LEDs used in this setup are fabricated by Nichia company having a color temperature of 5000 K while providing 4.16 W electrical power. The angle of radiation is specified as 120° and therefore suitable for uniform illumination. Based on experimental results those LEDs are also suitable to produce sharp shadows, which is the most important criterion when segmenting the shadow contours from the background. The illumination is a combination of two separate rings, the lowermost ring consists of eight LEDs arranged equally spaced to illuminate the specimen from a flat angle as shown in Figure 1.4(c).

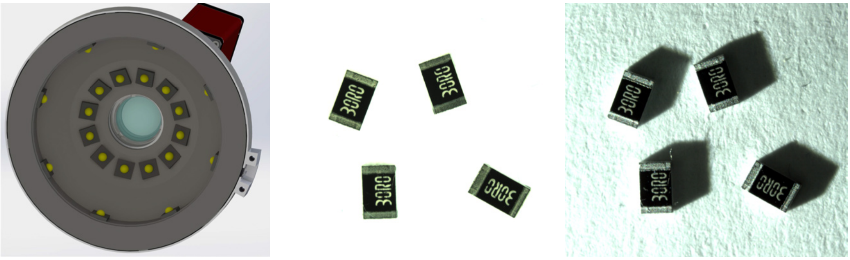

(a) Ringlight with LED rings (b) Overview image (c) Shadow demonstration

Figure 1.4: The illumination ring consists of two separately controllable LED rings (a). It can be used for uniformly illuminated overview images (b), while the lower ring produces sharp shadows (c).

This ring is used for generating the shadow contours. An upper ring is utilized to acquire homogeneous illuminated overview images (Figure 1.4(b)).

The second component is an industrial color camera Manta G-419C of ALLIED Vision Technologies with a resolution of 2048×2048 pixels. In our experiments the color sensor is not used. Segmentation and shadow detection is computed on the gray-scale image only. This camera was combined with the bi-telecentric objective TC 2M HR 016-C manufactured by Opto Engineering. The setup allows a pixel size of $4.5\ \mu\mathrm{m}^2$ and a depth of view of $2.0\ \mathrm{mm}$. Therefore the field of view is $9.2 \times 9.2\ \mathrm{mm}^2$. In order to scan larger surfaces, this setup can be extended with a motorized stage as shown in [FSB15]. The software implementation, which consists of the shadow detection, calibration and 3D estimation, was realized in C++ using the opencv image processing library [Bra00].

2 Algorithm and implementation

Essential to the 3D reconstruction is a robust calibration. In the initial algorithm step an estimation of the light positions $\boldsymbol{L}_i$ in three-dimensional space is computed. Our coordinate-system fixates the center point $\boldsymbol{p_c} = \left(c_x,\ c_y,\ z\right)^T$ of the spanned vector space $\mathbf{0}$ at the center of the projected image scene. The unit of this vector is *pixel* in the x and y dimension. The z dimension is a scalar value mapped to a metric scale by comparing to ground-truth height measurements or a-priori known height measurement of a common specimen, acquired with a standardized microscope. We furthermore assume a punctual light source $\boldsymbol{L}_i$ and a list of correspondences $C_i = \{c_{jk}\}$ with $|C_i| \geq 2$, c_{jk} representing a point on the object $\boldsymbol{o_j}$ and a corresponding shadow contour point $\boldsymbol{s_k}$. It is possible to construct equations of lines $l(c_{jk})$ with $\boldsymbol{o_j}$ as support vector and $t \cdot (\boldsymbol{s_k} - \boldsymbol{o_j})$ with $t \in \mathbb{R}$ as the direction vector. The light source $\boldsymbol{L}_i$ can then be estimated by finding the intersection points by pairwise constructing lines $l(c_{jk})$ and $l(c_{j'k'}), j' \neq j, k' \neq k$. Because of deviations when computing the corresponding points a single intersection point might not necessarily exist. Therefore the problem is solved by finding the point $\boldsymbol{p}$ with minimal euclidean distance to all given lines out of C_i, donated as $dist(\boldsymbol{p}, l)$ to yield an estimation for $\boldsymbol{L_i}$. In a next iteration to this optimization problem outliers, lines that increase the variance of the distance deviation, can be filtered out to compensate incorrectly mapped correspondences. The non weighted optimization problem, where every correspondence has the same influence on the estimation position of $\boldsymbol{L_i}$ is provided as follows:

$$\boldsymbol{L}_i = \arg\min_{\boldsymbol{p}} \sum_{\substack{j,k \\ j \neq k}} dist(\boldsymbol{p}, l(c_{jk}))$$

An example correspondence mapping is shown in Figure 2.1(a). The calibration needs to be estimated for all LEDs in the given setup. To find the correspondence points, knowledge of the light source's position can be incorporated. It is helpful to choose simple specimens for calibration. In our example the corresponding points could be estimated by using a Harris corner detector as shown in [BPLF12] and [GW08]. In combination with the overview image Figure 1.4(b) corner candidates located on the object and others introduced by shadow can be distinguished as those appear in both images. False positives can be eliminated by taking previously known symmetric constraints into account. As the calibration is a crucial part concerning the accuracy of this method a manual calibration, implemented as a wizard in software is highly recommended. Figure 2.1(b) illustrates the algorithm for determining the height value at different positions (red circles) on the image plane. The outer contour of a shadow area S_i introduced by LED $\boldsymbol{L}_i$ can be estimated by masking the segmented specimen itself with the post-processed overview image Figure 2.2(b). After applying a threshold to segment the shadow from the background the contour can be estimated by computing its outline with morphological operators and edge detection. As we are only interested in those parts of the outer boundary, that have at least a minimum

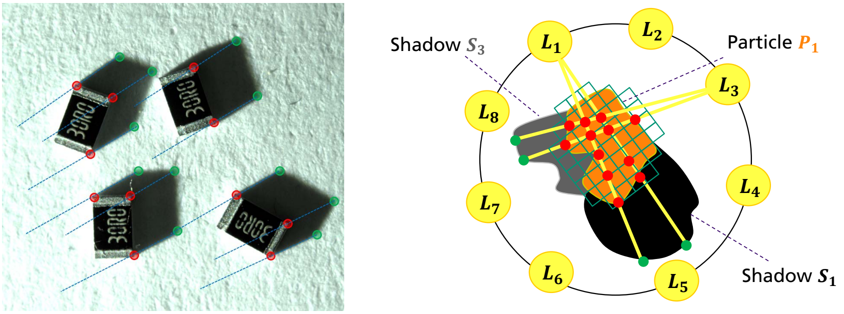

(a) Ringlight (b) overviewlights

Figure 2.1: Correspondences object (red) and shadow points (green) are maintained in a correspondence list C_i (a). The height at every position on the object is iteratively estimated through LED $\boldsymbol{L_i}$ and shadow boundary points B_i by finding the minimum z-value (b).

distance from the specimen itself in the direction of light position, those non relevant candidates are removed by multiplying the contour image with a slightly enlarged mask. The result can be seen in Figure 2.2(a). With the position of $\boldsymbol{L}_i$ and the shadow boundary points $B_i = \{s_0, \ldots, s_n\}$, containing all shadow points s_n produced by the light source out of the direction $\boldsymbol{L}_i$, a height value can be assigned to every pixel position $\boldsymbol{q} = \left(x,\, y,\, 0\right)^T$ on the image plane. The height value is computed by an orthogonal projection of the lines of sight $l_{ii}(\boldsymbol{L}_i, B_i)$ between the LED $\boldsymbol{L}_i$ and all corresponding shadow boundary points B_i as shown in Figure2.1(b). This procedure is repeated for all calibrated LEDs in this setup. While computing the height values produced by a single light-source $\boldsymbol{L_i}$ a maximum rule is assumed, which means that a larger height value is kept. This cares for artifacts introduced by the assumption of a point light source, which would produce borders of the specimen with a height h of zero, because the shadow path starts right next to the edge of the specimen. This maximum rule is only applied if there was no better height, e.g. lower height assigned by another light-source $\boldsymbol{L_j}$. That means, height values assigned by the computation of a different light-source are evaluated by maintaining a minimum rule. The height value h' at position $\boldsymbol{q'}$ is therefore only updated whenever the new height value is lower than the current value, which assigned by different light-source. The algorithm iterates over all light-sources, starting with on randomly selected light. The order does not matter, but every light and corresponding shadow points are only evaluated once. The line is constructed from the direction of the light-source and ends on the particle filter with height $z = 0$. After the iteration is finished the mask computed in a prior step multiplied by the image to eliminate artifacts located outside of the object.

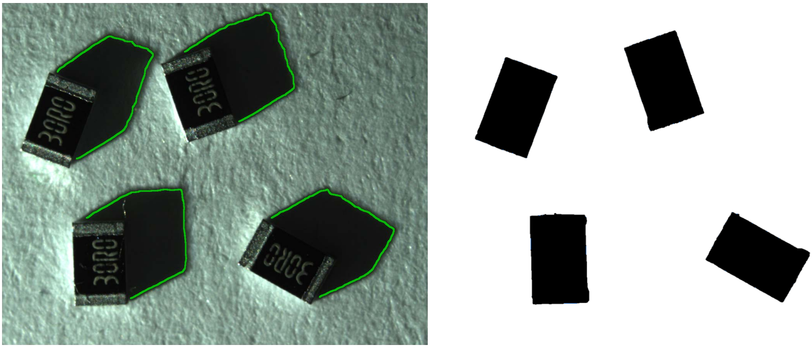

(a) (b)

Figure 2.2: Outline is extracted by image processing algorithms (a). A mask is computed for later segmentation of the resulting height estimation (b).

3 Results

When directly comparing the results with measurements acquired by a professional system as illustrated in Figure 3.1(a) one can directly see that the height resolution of the microscope is much higher than the reconstruction seen in Figure 3.1(b) and 3.1(c). The microscope reconstructs the surface in much greater detail, taking properties of the surface like roughness into account. As seen on the result images, initial calibration yields results that fit into the expected range of the values measured before. The chip and its cuboid shape are accurately reconstructed. The height, which is specified at around 6 mm according to the data-sheet is in the same range as the height computed by the presented method. When looking at Figure 3.1(c), it becomes evident that the calibration needs to be optimized as currently single outliers in the list of corresponding points result in a displacement of the estimated LED position, which directly influences height estimation. Another point for improvement is the shadow edge detection, as single artifacts worsen the measurement results. This cannot alone be achieved by changing the edge detection algorithms or further post-processing but needs to be incorporated into a model approach which uses sanity checks to remove falsely detected contours. As shown in Figure 3.1 on flat objects, that are known before hand, these calibration errors can be corrected after the reconstruction by averaging the height values. But for rough surfaces, this compensation approach will lower the reproduction granularity of the surface and therefore the height resolution will be further reduced. Hence it is suggested to reduce possible errors in each image processing step. When comparing the given results with the microscope's measurement one can see, that the height dimensions are in a similar range but still way off when micrometer accuracy is required. A really big advantage of the donated setup is the large lateral range $1000 \times 1000\ \mu\mathrm{m}^2$ that can be measured without stitching partial results together.

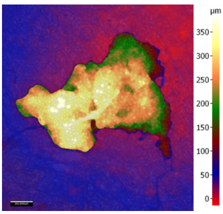

(a)

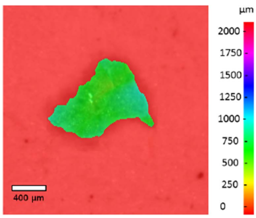

(b)

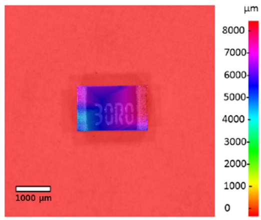

(c)

Figure 3.1: Alicona's InfiniteFocus reconstruction with clear surface details (a) and reconstructions estimated with the methods presented in this report (b) and(c).

4 Conclusion and discussion

There are two critical parts in this setup. The first part is for sure the initial calibration of the experimental setup, which will be examined in future research. The other critical part is the estimation of the shadow boundaries, because these directly influence the height estimation. In the presented approach every pixel is used with the same weight, meaning every pixel has the same impact in the algorithm to estimate the height values. As seen in Figure 4.1 the algorithm is very sensitive to noise. Every pixel, that is segmented from the background is directly added into the boundary list B_i and therefore used for computing the height-value. As of now there is no regularization that could work around wrongly detected pixels or noise. Figure 4.1(c) especially shows that noise will highly influence the measurement. As the noise has a large impact on the error, this issue violates the conditions of a well-posed problem, according to [Rie03] the given problem is ill-posed out of that reason. Future methods therefore need to propose a way for regularization. This could be by defining proximity rules for boundary pixel within a neighborhood. Fixating the area around a particle out of given geometric preconditions and the already known light position $\boldsymbol{L_i}$ is also suggested.

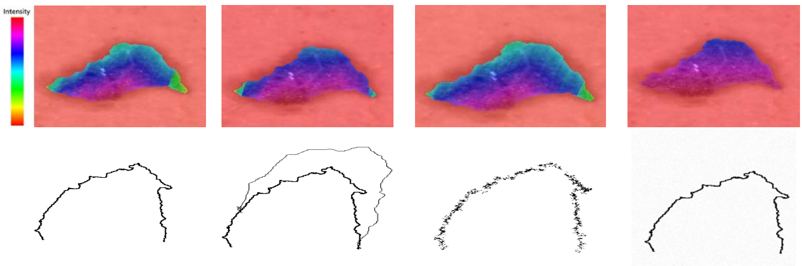

(a) (b) (c) (d)

Figure 4.1: From left to right the original contour (a) produced by $\boldsymbol{L_6}$ was modified by extending the original contour (b), adding noise around the contour (c) and by adding noise onto the complete image (d). All images are colored with the same color scale. All images use the same color-map and are directly comparable.

Besides the issues concerning robustness, the approach shown in section 2 is already producing results. It was implemented as a software and hardware prototype with the goal to realize a cost-efficient sensor for estimating height and volume information of dirt particles. As demonstrated in section 3, it is possible to estimate this information with a quite simple setup. In the future, these results need to be further compared and benchmarked in detail against ground-truth measurements to determine the accuracy and robustness of this approach. On the qualitative side the introduced model should also be extended by surface properties like roughness or material characteristics to improve the height estimation. The artifacts introduced by assuming a linear relation between shadow contour candidate, the point light position and the resulting height could be post-processed by introducing these surface characteristics.

Estimating height information while maintaining high-throughput measurements in the context of an industrial in-line QA process is still a critical task today. Hence a huge demand for measurement systems, that can ensure persistence in industrial environments while also keeping service costs low exists. The solution shown in this paper yields great potential for those kind of systems in the near future.

Bibliography

[BPLF12] Jürgen Beyerer, Fernando Puente León, and Christian Frese. *Automatische Sichtprüfung: Grundlagen, Methoden und Praxis der Bildgewinnung und Bildauswertung*. Springer Vieweg, 2012.

[Bra00] G. Bradski. *Dr. Dobb's Journal of Software Tools*, 2000.

[dA14] Verband der Automobilindustrie. *VDA Band 19 Püfung der Technischen Sauberkeit – Partikelverunreinigung funktionsrelevanter Automobilteile*, 2014.

[FKB14] Peter Frühberger, Edmund Klaus, and Jürgen Beyerer. Microscopic analysis using gaze-based interaction. volume 154 of *Springer Proceedings in Physics*, 2014.

[FSB15] Peter Frühberger, Thomas Stephan, and Jürgen Beyerer. Integrating microscopic analysis into existing quality assurance processes. volume 164 of *Springer Proceedings in Physics*, 2015.

[FSB16] Peter Frühberger, Thomas Stephan, and Jürgen Beyerer. Estimating 3d-volume of dirt particles using depth from shadow. volume 174 of *Springer Proceedings in Physics*, 2016. forthcoming.

[GW08] Rafael C. Gonzalez and Richard E. Woods. *Digital Image Processing*. Pearson International Edition, 3 edition, 2008.

[Rie03] Andreas Rieder. *Keine Probleme mit Inversen Problemen : eine Einführung in ihre stabile Lösung*. Vieweg, Wiesbaden, 1. aufl. edition, 2003.